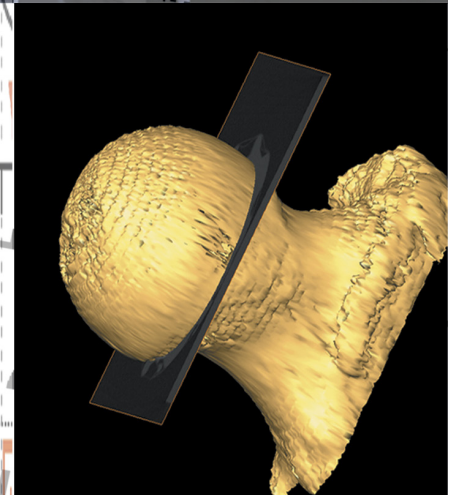
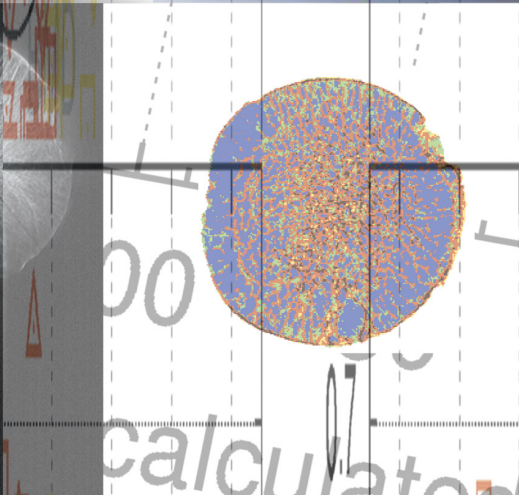
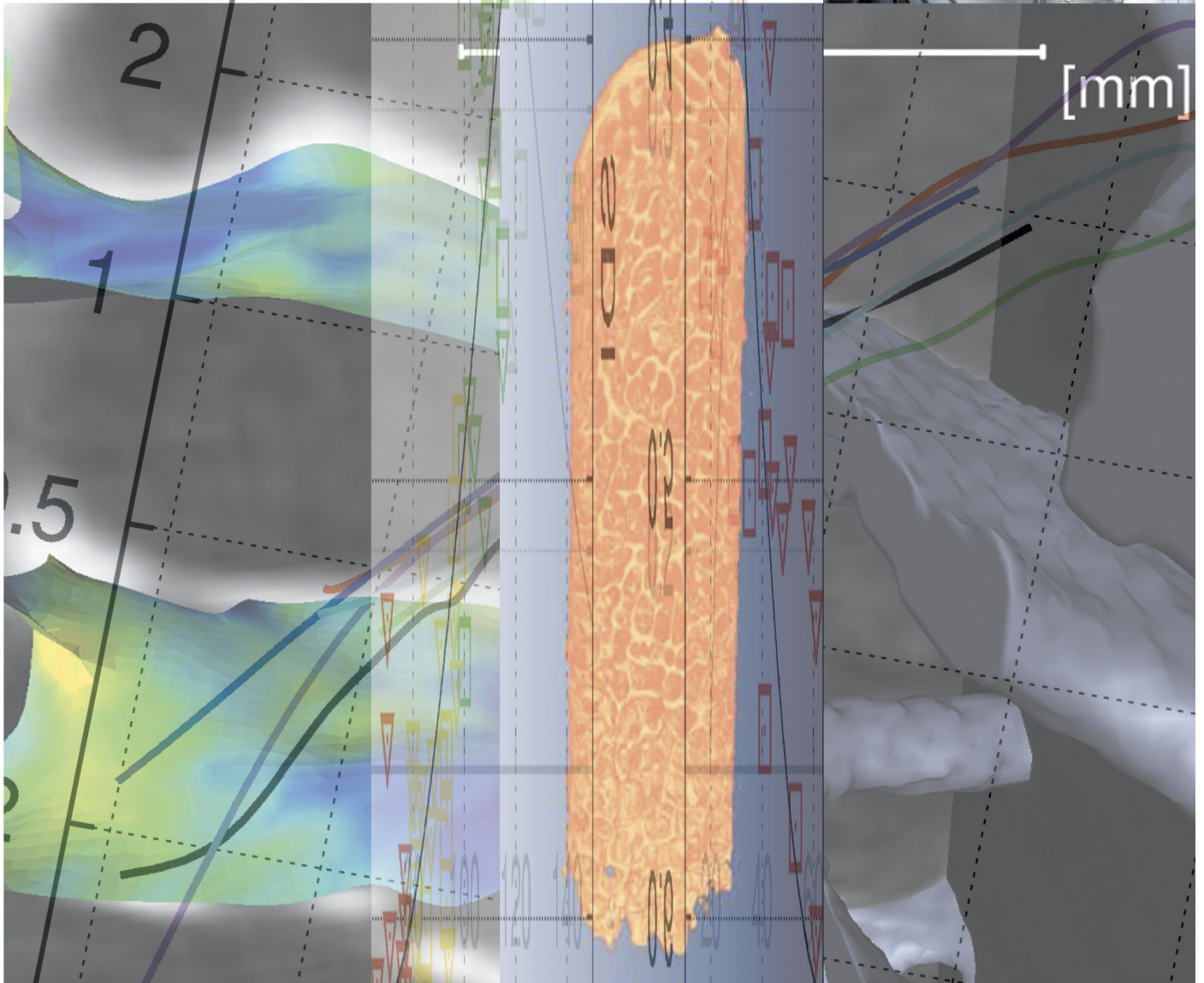


# 2D and 3D Quantification of Bone Structure and its Changes in Microgravity Condition by Measures of Complexity

<http://bone3D.zib.de>

**Final Report (2 years)**

**Project Acronym: Bone 3D**



## Table of Contents

Table of Contents .....	1
Foreword .....	2
Acknowledgements .....	3
Project Team .....	4
Abbreviations and Glossary .....	5
BONE3D Goals .....	6
Focus .....	6
First Phase Focus .....	6
Introduction .....	7
Prospects .....	8
Scientific Impact .....	8
Scientific Background and Perspectives .....	9
BONE3D Results First Phase .....	13
Computer Set-Up at FUB .....	13
Collection of Specimens and Their Preparation .....	13
Imaging of 180 Bone Specimens and BMD Measurements .....	13
pQCT Imaging .....	13
Slice location definition .....	14
Phantom Tests Performed on pQCT .....	14
BMD-Measurement of Lumbar Spines .....	14
QCT of the Femoral Neck .....	14
Radiography .....	15
Image Resolution and Measures of Complexity .....	15
Measures of Complexity for 2D Images from Different Skeletal Locations .....	15
Bone Modeling .....	19
Acquiring Bone Biopsies from Human Tibiae Specimens .....	20
Preparation of the Tibia Biopsies for $\mu$ -CT Scanning .....	20
3D Scanning of Tibia Biopsies .....	21
Damage Assessment and Identification of Potential Artifacts in Biopsies .....	21
Quantification of the Trabecular Bone Structure with Traditional 2D Histomorphometry – Relationship to 3D $\mu$ -CT evaluation .....	23
Appropriateness to Use $\mu$ -CT Data Sets for 3D Measurements of Complexity .....	26
Skeletonization of the Trabecular Network and Other Visualization Tools as a Basis for Structural Quantification .....	27
Measures of Complexity to Quantify the 3D Structure of Bone .....	28
Views and Recommendations from the Industrial Partners .....	33
Siemens AG .....	33
Scanco Medical AG .....	33
Publications .....	34
Scientific Publications .....	34
Oral Presentations at Conferences .....	35
Poster Presentations at Conferences .....	35
Other Scientific Work .....	35

## Foreword

This Final Report represents the achievements of the research Project “2D and 3D Quantification of Bone Structure and its Changes in Microgravity Condition by Measures of Complexity”. The short form of the project title is “Bone3D”.

This project started at the end of December 2000. The reporting time span is two years until the end of 2002. The project is an ESA project under MAP AO-99-030. The ESTEC contract number is 14592/00/NL/SH.

The website of the project <http://bone3D.zib.de> contains information that cannot be shown in print. The visitor will be able to see movies showing 3D data of human bone biopsies acquired by micro-computed tomography.

The abstracts of publications are provided in this report. Full papers are available to the interested reader by contacting the author, a library, or the journal. More publications are in preparation at this point of time (December 2002/January 2003).

**The motto of the team has been to follow the success of Pioneer 10 as a shining example for this project.**

## Acknowledgements

The project was funded partly by the European Space Agency; Siemens AG (Germany); Scanco Medical AG (Switzerland); and F. Hoffmann-La Roche Ltd, Pharmaceuticals Division (Roche Pharmaceuticals) (Switzerland), the Center of Muscle and Bone Research at the University Hospital Benjamin Franklin (Berlin, Germany), the Free University Berlin, the University of Potsdam (both Germany), the Konrad-Zuse Institute Berlin (Germany), and the University of Aarhus (Denmark).

The scientific team members are grateful for the financial support they received. Despite the financial involvement of the industrial partners Siemens AG and Scanco Medical AG, the industrial support received was outstanding and made this project successful.

The personal involvement of Dr. Roger Binot (technical officer) from ESTEC, as well as from the administrative officer Mrs. Soisick Hamon, is greatly acknowledged and brought the communication between ESA and the project partners to a comfortable level of mutual understanding.

The Institute of Anatomy of the Free University Berlin (Prof. R. Graf) and the Institute of Anatomy of the Humboldt University in Berlin (Prof. G. Bogusch) provided the human bone material essential for the project. The team is very thankful for the support, without it this basic research project would not have achieved its goals. The assistance in technical matters by Prof. Bogusch and the help of the anatomical lab technicians were invaluable at the beginning of the project.

The involvement of Hewlett-Packard (Germany) in the basic configuration of the set-up and linkage of several new electronic components was thankfully received by the team members at the Free University Berlin.

The team thanks the radiological technicians Erika May, Martina Kratzsch, and Frank Touby at the University Hospital Benjamin Franklin for their work. In particular, Erika May made it possible to finish all radiological examinations of bone specimens in line with the time schedule of this project.

The technical department at the University Hospital Benjamin Franklin (Mr. Forster, Mr. Bräuer) helped always in time to solve technical problems with laboratory equipment and the set-up requirements for radiological examinations.

Birthe-Gyilling Jørgensen and Inger Vang Magnussen, Institute of Anatomy, University of Aarhus, are gratefully acknowledged for their skilled assistance in preparing the histological sections.

The title page was created by August Zimmermann, Berlin. We are grateful for his work and for his patients to go through many discussions before the final design was achieved.

## Project Team

The overall budget for the two years of this project was €1.278.900. ESA funded €466.000, the industrial partners €138.000, and the project user group €51.000. The remaining €623.900 were contributed in cash and/or in-kind by the academic partners.

<b>Technical Officer</b>	ESA/ESTEC	Noordwijk	The Netherlands	Dr. R. Binot
<b>Project Coordinator</b>	FUB	Berlin	Germany	Dr. W. Gowin
<b>Academic Partners</b>	FUB	Berlin	Germany	Dr. W. Gowin Dr. P. Saporin Dr. M. Giehl A. Boshof, M.S. Prof. D. Felsenberg
	ZIB	Berlin	Germany	H.-C. Hege, M.S. S. Prohaska, M.S.
	UoP	Potsdam	Germany	Prof. J. Kurths Dr. A. Zaikin
	UoA	Aarhus	Denmark	Prof. L. Mosekilde † Dr. J. S. Thomsen
<b>Industrial Partners</b>	Siemens	Forchheim	Germany	Dr. K. Klingenberg-Regn
	Scanco	Zürich	Switzerland	Dr. B. Koller
<b>Project User Group</b>	Roche Pharmaceuticals	Basel	Switzerland	
	Hewlett-Packard	Hamburg	Germany	

FUB	Free University Berlin, University Hospital Benjamin Franklin, Center of Muscle and Bone Research (former Osteoporosis Research Group)
ZIB	Zuse Institute Berlin, Dept. of Scientific Visualization
UoP	University of Potsdam, Institute of Physics, Nonlinear Dynamics
UoA	University of Aarhus, Institute of Anatomy, Dept. of Cell Biology
Scanco	Scanco Medical AG
Siemens	Siemens AG, Div. Medical Equipment

### **Project coordinator contacts:**

Wolfgang Gowin, MD, PhD

Phone: +49-30-8445-4617

Fax: +49-30-8445-4539

E-Mail: [wolf1234@cipmail.ukbf.fu-berlin.de](mailto:wolf1234@cipmail.ukbf.fu-berlin.de)

## Abbreviations and Glossary

First phase	Relates to the first two years of this research program (= period of time of this report)
ISS	International Space Station
BMD	Bone mineral density
QCT	Quantitative computed tomography
pQCT	Peripheral quantitative computed tomography
Amira	Software platform for 3D data analysis, visualization, and quantification
$\mu$ -CT	Micro-computed tomography
FOV	Field of View
<u>2D images:</u>	
ROI	Region of Interest
L, V, H, I, C	Symbols used to encode pixels of 2D image: Lake, Valley, Highland, Incline, Cliff
IGE	Index of Global Ensemble: $IGE = [p(I)+p(C)] / [p(L)+\epsilon]$
SCI	Structure Complexity Index: entropy of the distribution of local quantities $SCI = - \sum p_{ile} \log p_{ile}$ , where local quantity $ILE = [p_{local}(I)+p_{local}(C)] / (p_{local}(L)+\epsilon)$ and $\epsilon = 10^{-3}$ is a tiny constant to avoid division by zero.
SDI	Structure Disorder Index, Shannon Entropy of 3D distribution of the triplets $\{p(L), p(I, C), p(V, H)\}$
TNI	Trabecular Network Index, $TNI = \text{median}(p_{tr}) / (S(p_{tr}) / S_{max})$ , $p_{tr}=p(V)+p(I)+p(C)$
Max L-block,	Size of maximal connected soft area composed by symbol L
Mean L-block	Average size of connected soft areas composed by symbol L
<u>3D images:</u>	
VOI	Volume of Interest
M, S, I	Symbols used to encode voxels of 3D image: Marrow voxel, Surface bone voxel, and Internal bone voxel
Normalized Entropy	3D entropy of geometrical locations of bone voxels normalized by the value of maximal entropy for the given partition of a 3D VOI
BV/TV	Bone Volume to Total Volume ratio calculated from 3D data
SCI 3D	Structure Complexity Index for 3D data: entropy of the distribution of local quantities $SCI_{3D} = - \sum p_{ILE_{3D}} \log_2(p_{ILE_{3D}})$ , where $ILE_{3D} = [p_{local}(S)+p_{local}(I)] / [p_{local}(M)+\epsilon]$
SCI(BV/TV)	Structure Complexity Index of local BV/TV distribution. Uses local BV/TV from the moving cubic window as a local quantity
SurfCI	Surface Complexity Index: entropy of distribution of local surface indexes introduced as $p_{local}(S) / [p_{local}(I)+p_{local}(S)]$
BSV/BV or SurfIGE	Surface Index of Global Ensemble calculated as ratio between the volume occupied by bone surface voxels, and the total bone volume: $SurfIGE = p(S) / [p(I)+p(S)]$

## BONE3D Goals

### Focus

- ✚ Development of a diagnostic program for the quantification of structural changes within the microarchitecture of human bones based on radiological procedures:
  - ⊕ The quantification of the changes in the architecture is based on measures of complexity derived from nonlinear dynamics which are applied to modern radiological imaging modalities.
  - ⊕ Architectural skeletal discordance is accounted for by evaluating several skeletal regions.
  - ⊕ The diagnostic program should be applicable to space-flying personnel as well as to patients on earth.
  - ⊕ The diagnostic program should be configured in such a manner that appropriate countermeasures for treatment or prevention can be concluded from the results.
  - ⊕ The success or failure of the countermeasures can be monitored with the diagnostic program.

### First Phase Focus

- ✚ Development of a method for non-invasive evaluation of the bone structure using 2D quantitative computed tomography images based on human specimens acquired at different skeletal sites,
- ✚ development of a procedure for the precise quantification of a 3D bone architectural composition by analyzing human bone biopsy data sets obtained by  $\mu$ -CT,
- ✚ testing of the new measures on paradigmatic mathematical and physical models.

## Introduction

The objective of the research program is to establish a precise diagnostic method for the quantification of changes in bone structural composition. The project develops the tools to evaluate structural loss in bone architecture and gains new quantitative information about the bone metabolism in microgravity condition. This evaluation is mostly based on symbolic dynamics and measures of complexity derived from the field of nonlinear dynamics.

The most precise procedure for diagnosing structural alterations will be developed and scientifically proven through the research project. The outcome of such comprehensive diagnostic program will provide the fundamental basis for monitoring, prevention, and treatment of structural changes of the bone in microgravity condition. This will have an impact on astronauts and other space-flying personnel working on the ISS in the future, and for patients with bone metabolic diseases on Earth.

The following tasks have been solved during the first phase of the project:

- ✚ development of a method for non-invasive evaluation of the bone structure using 2D quantitative computed tomography images based on human specimens acquired at different skeletal sites,
- ✚ development of a procedure for the precise quantification of a 3D bone architectural composition by analyzing human bone biopsy data sets obtained by  $\mu$ -CT,
- ✚ the new measures were tested on paradigmatic mathematical and physical models,
- ✚ validation of the findings by comparison of the  $\mu$ -CT-outcome with static histomorphometric examinations.

During the first phase, the team of BONE3D submitted successfully a follow-up phase proposal for three years. The main objectives for the second phase of the project are:

- ✚ adjustment and refinement of the developed algorithms for numerical assessment of the changes in bone architecture based on noninvasive patient examinations at different skeletal sites,
- ✚ transfer of the methods for pre- and post-flight examination of space-flying personnel to quantify the rate of changes in bone composition caused by microgravity condition,
- ✚ further investigation and development of 3D parameters quantifying the architectural composition of the bone (measures of complexity, porosity, topological and geometrical defect measurements) based on human specimens of proximal tibia biopsies, and lumbar vertebrae,
- ✚ investigation of human iliac crest biopsies obtained from Russian probands before and after bed rest studies,
- ✚ investigation and development of an ultrasound derived structural parameter,
- ✚ continuous development of 2D and 3D bone models for the application to predict the susceptibility of bone structural deterioration during space flight.

## Prospects

After the successful completion of the research program the prospects will be:

- ✚ Microgravity effects on bone can be precisely quantified and monitored with the proposed technique.
- ✚ Crew persons may be selected by model-based predictions of their potential bone structure loss.
- ✚ The outcome of this research program will provide new information about bone metabolism and will lead to a better and quantified diagnosis for patients with bone diseases in general.
- ✚ The expansion of the technique of symbolic dynamics and measures of complexity to analyze 3D data will have a significant impact on nonlinear dynamics. It opens new prospects to analyze, quantify, and compare numerically different aspects of structural organization when the information of the underlying model is not available.
- ✚ An integrated 3D working environment will be available offering new powerful methods for analyzing and visualizing complex 3D image data for quantitative bone assessment.

## Scientific Impact

The results of this project will have an impact in the following areas:

- ✚ Health care for space-flying personnel.
- ✚ Health care for patients with bone diseases on Earth.
- ✚ Theoretical physics, signal and image analysis, biomedical science, material science.
- ✚ Scientific visualization, image data analysis, and management of large data sets.

## Scientific Background and Perspectives

Non-destructive and non-invasive examinations of the human bones can only be performed with the application of radiological procedures. Pathological alterations of the bone appear as changes in radiological density and as changes of the structure. Changes of density can be quantified by several osteodensitometric methods. The QCT represents the gold standard of all osteodensitometric approaches [1].

The two methods to evaluate the structure of the bone are the histomorphometric approach to examine bone biopsies [2], and biopsy examinations by recently developed  $\mu$ -CT devices [3]. The former approach is of invasive nature and destructive for the biopsy and therefore not repeatable, the latter is invasive as well; however, the biopsy can be studied repeatedly as long as the material is preserved properly.

The current standard for evaluating the structure of bone is histomorphometry [4]. Recent advances use a digital image of the thin bone section which is analyzed by an automated computer program [5]. These 2D analyses allow the evaluation of the bone volume, cortical width, trabecular thickness, trabecular separation, trabecular number [6]. Trabecular connectivity density [7] and star volume [8] are more advanced measurements among others [9,10]. However, all parameters derived from microscopic examination of thin bone sections are limited as they are localized expressions of the structural arrangement within a two-dimensional plane. There is thus not necessarily a close correlation between the 2D and 3D bone structure. Moreover, the structural elements of the bone are arranged in three dimensions and the architectural composition is based on the direction of the applied load. This can result in dramatic differences of spatial arrangement of these structural elements within very short distances.

To overcome the inherent difficulties of histomorphometry, the radiological method of  $\mu$ -CT has been applied to examine bone samples [11-13]. Biopsies can be examined without destruction of the sample. Slices with the same thickness as histological sections can be produced and analyzed by conventional histomorphometry parameters. 3D reconstruction of the data resembles the biopsy itself. True assessments of the 3D architecture are possible only with 3D data sets acquired by  $\mu$ -CT. The architectural composition of a complex porous material such as bone may be assessed with different measures which evaluate its homogeneity, the regularity, the degree of order or disorder, and its complexity. Such assessments would result in a quantification of the architecture as a whole (3D) still including the single parts it is built from.

Team members at FUB and UoP developed a new method based on the application of symbolic dynamics and measures of complexity which derive from the field of nonlinear dynamics [14]. This approach led to a set of quantitative 2D measures evaluating different aspects of the structural composition. The method utilizes routinely acquired skeletal QCT-images. The method has been successfully applied to assess patient data as well as different vertebral pathologies [15,16]. The results demonstrate clear distinction of the architecture of normal, osteopenic, and osteoporotic bones and quantify its differences. Normal trabecular bone has a complex and ordered structure. Osteopenic bone is disordered and has a significantly lower complexity, whereas osteoporotic bone exhibits a simple and ordered structure.

These measures of complexity provide non-invasive in vivo bone structure assessment. Patients or space-flying personnel who need an evaluation of their bone density by QCT receive the structure assessment without additional radiation exposure, since this method is a supplementary evaluation of the QCT-image.

The development of measures of complexity expanded the application of nonlinear dynamics in medicine [17]. The current trends in the field of nonlinear dynamics include the development of methods analyzing complex experimental data derived from different fields of science. Such new methods are tested on paradigmatic systems for which mathematical models and behaviors are known. Recently, the quantification of complexity in hierarchical systems became an interdisciplinary task which requires a flexibility of operation leading to the introduction of new context-dependent derivatives and to a constant interaction with the theoretical aspects of the definition of complexity itself. The need of further research in this area is inevitable [18].

Current trends in the field of radiological assessment of bone structure and microarchitecture are the refinement and further development of the  $\mu$ -CT technique [19,20], and the development of fast high-resolution spiral CT-scanners. The  $\mu$ -CT technique is being improved by cone beam technology, variation of sample size up to 5 cm in diameter, refinement of the resolution down to 10  $\mu$ m, and multi-slice techniques [21].

Spiral CT-scanners providing fast acquisitions and high-resolution images are now being marketed. Such scanners were not available at the beginning of the project. The team will have access to such a scanner at FUB and will further develop vertebral imaging together with Siemens AG in order to achieve 2D high-resolution and 3D bone structure quantification based on measures of complexity in patients. The new vertebral CT-imaging protocols need to be investigated on the basis of human lumbar specimens, their 3D assessment of the structural composition by  $\mu$ -CT, their histomorphometric results, and their biomechanical failure load. These tasks have not been performed yet and will be subject of the second phase of this project. The result will be a thoroughly tested examination protocol for vertebral bone status assessment including both BMD and structure quantification.

Alternative skeletal regions for bone structure assessment have been studied. This project came to the conclusion that the proximal tibia metaphysis is easily accessible and a reliable location for such measurements. Peripheral skeletal locations have been investigated and are considered for patient application.

The most precise structure evaluations have been made on iliac crest bone biopsies. Histomorphometric tools have been applied in the past. Current knowledge and technological advancement imply the usage of  $\mu$ -CT for such evaluations. Although the iliac crest is easily accessible, it is a non-weight bearing bone and, therefore, a questionable skeletal location for structure assessment in space-flying personnel. This team has developed the procedure to assess bone biopsies derived from the equally accessible region of the proximal tibia. Comparisons and synoptic approaches are needed to make a decision which skeletal region is the most appropriate for bone structure assessment and monitoring. The loss of structure and mass in bone during microgravity exposure can be quantified with these methods as they are currently developed by this team.

Mathematical and physical models of bone behavior have been described. The data assembled from human skeletal specimens and patients in this project will be used to build refined and new models for 3D and 2D bone status assessment. It is a goal of the space agencies to identify individuals which are vulnerable to osteoporosis. The consideration of selecting crew personnel based on the prediction of the susceptibility to bone structure loss and bone mass loss is a strategic goal. Moreover, the determination of countermeasures for bone loss must be based on monitoring the changes in bone in microgravity. The application of models already

developed by the team might be an important tool for such tasks. Most certainly, the models need refinement and rigorous testing.

The dramatically increased quality of imaging and the availability of 3D data require a tool for the analysis and quantification of the bone architecture based on these 3D data. Amira is a platform providing state-of-the-art image analysis and visualization techniques. It is an extendable programming environment. In this way bone specific assessment algorithms can be integrated and tested. Due to the increasing size of data in all fields of scientific imaging, handling of such data sets with Amira will be improved in the future. One way is to use larger computers and run a 64-bit version. Another way is to use external memory algorithms running with a small amount of main memory, while the main part of the data is stored only on disk. Both ways are explored by the Amira developing team. A 64-bit beta version is available to the project partners. The current version of Amira (3.0) provides a basic interface allowing on-disk-processing of data. The development of external memory algorithms is ongoing and of major scientific interest. The evaluation of 3D bone architecture requires new image visualization and analysis techniques, as elaborated in the past and for the future of this project

#### References for this chapter:

1. Guglielmi, G., Lang, T.F., Cammisa, M., Genant, H.K.: Quantitative computed tomography at the axial skeleton. In: H.K. Genant, G. Guglielmi, M. Jergas (eds.): Bone densitometry and osteoporosis. Springer Verlag, Berlin, 1998, 335-347
2. Parfitt, A.M., Mathews, C.H.E., Villanueva, A.R., Kleerekoper, M.: Relationships between surface, volume, and thickness of iliac trabecular bone in aging and in osteoporosis. *J Clin Invest* 72, 1983, 1396-1409
3. Rüegeegger, P., Koller, B., Müller, R.: A microtomographic system for the nondestructive evaluation of bone architecture. *Calcif Tissue Int* 58, 1996, 24-29
4. Chavassieux, P., Arlot, M., Meunier, P.J.: Clinical use of bone biopsy. In: R. Marcus, D. Feldman, J. Kelsey (eds.): Osteoporosis. Academic Press, San Diego, 1996, 1113-1121
5. Roux, J.P., Arlot, M., Gineyts, E., Meunier, P.J., Delmas, P.D.: Automatic-interactive measurement of resorption cavities in transiliac bone biopsies and correlation with desoxypyridinoline. *Bone* 17, 1995, 153-156
6. Parfitt, A.M., Drezner, M.K., Glorieux, F.H., Kanis, J.A., Malluche, H., Meunier, P.J., Ott, S.M., Recker, R.R.: Bone histomorphometry: Standardization of nomenclature, symbols and units. *J Bone Miner Res* 6, 1987, 595-610
7. Garranhan, N.J., Mellish, R.W.E., Vedi, S., Compston, J.E.: A new method for the two-dimensional analysis of bone structure in human iliac crest biopsies. *J Microsc* 142, 1986, 341-349
8. Vesterby, A., Gundersen, H.J.G., Melsen, F.: Star volume of marrow space and trabeculae of the first lumbar vertebra: Sampling efficiency and biological variation. *Bone* 10, 1989, 7-13
9. Gundersen, H.J.G., Boyce, R.W., Nyengaard, J.R., Odgaard, A.: The Conneuler: Unbiased estimation of connectivity using physical disectors under projection. *Bone* 14, 1993, 217-222
10. Thomsen, J.S., Ebbesen, E.N., Mosekilde, L.: Relationships between static histomorphometry and bone strength measurements in human iliac crest bone biopsies. *Bone* 22, 1998, 153-163
11. Feldkamp, L.A., Goldstein, S.A., Parfitt, A.M., Jasion, G., Kleerekoper, M.: The direct examination of three-dimensional bone architecture in vitro by computed tomography. *J Bone Miner Res* 4, 1989, 3-11
12. Kinney, J.H., Lane, N.E., Haupt, D.L.: In vivo three-dimensional microscopy of trabecular bone. *J Bone Miner Res* 10, 1995, 264-270

13. Bonse, U., Busch, F.: X-ray computed microtomography ( $\mu$ CT) using synchrotron radiation. *Prog Biophys Mol Biol* 65, 1996, 133-169
14. Sapiro, P.I., Gowin, W., Kurths, J., Felsenberg, D.: Quantification of cancellous bone structure using symbolic dynamics and measures of complexity. *Phys Rev E* 58, 1998, 6449-6459
15. Gowin, W., Sapiro, P., Kurths, J., Felsenberg, D.: Order, disorder, and complexity of vertebral bone architecture. *Bone* 23, 1998, Suppl., S635
16. Gowin, W., Sapiro, P., Kurths, J., Felsenberg, D.: Complexity of bone architecture: A new method to assess structure. *Osteoporosis Int* 8, Suppl. 3, 1998, 87
17. Kurths, J., Voss, A., Sapiro, P., Witt, A., Kleiner, H.J., Wessel, N.: Quantitative analysis of heart rate variability. *Chaos* 5, 1995, 88-94
18. Schreiber, T.: Interdisciplinary application of nonlinear time series methods. *Phys Rev Lett* 308, 1999, 1-64
19. Engelke, K., Kalender, W.: Beyond bone densitometry: Assessment of bone architecture by x-ray computed tomography at various levels of resolution. In: H.K. Genant, G. Guglielmi, M. Jergas (eds.): *Bone densitometry and osteoporosis*. Springer Verlag, Berlin, 1998, 417-447
20. Genant, H.K., Engelke, K., Fuerst, T., Glüer, C.-C., Grampp, S., Harris, S.T., Jergas, M., Lang, T., Lu, Y., Majumdar, S., Mathur, A., Takada, M.: Noninvasive assessment of bone mineral and structure: state of the art. *J Bone Miner Res* 11, 1996, 707-730
21. Engelke, K., Karolczak, M., Schaller, S., Lutz, A., Seibert, U., Gowin, W., Felsenberg, D., Kalender, W.A.: A flexible  $\mu$ CT system for the analysis of trabecular bone structure in vitro. *Bone* 23, 1998, Suppl., S521

## **BONE3D Results First Phase**

### **Computer Set-Up at FUB**

The project demanded a specific computer set-up for acquiring 3D data sets, visualization and quantification of these data, and storage. After consultations with SUN, Hewlett-Packard, IBM, and experts from the partner ZIB, the conclusion was reached to order three different computers where each has a specific task instead of buying a large computer handling everything. We received the best offer from HP (PC workstation for image data visualization, multiprocessor RISC 64-bit Unix workstation for computing of acquired data, Linux server for data storage and archive). The computers were delivered until the end of January 2001. The funds to purchase the computers and their peripherals were supplied by our industrial partner Siemens AG. Thereby, the financial commitment of Siemens AG was fulfilled on schedule to the full term of the contract.

The Amira framework, a 3D visualization and quantification software package developed by ZIB, is installed on computers at FUB since January 2001, on computers at UoP since September 2001, and has been updated constantly.

In order to fulfill this first task, the academic and industrial partners worked together without even minor problems.

### **Collection of Specimens and Their Preparation**

FUB collected from 30 human cadavers 6 bone specimens each (lumbar spine, proximal femur, calcaneus, distal tibia, distal radius, midshaft humerus) in February 2001. These specimens remain at FUB for the duration of the project. The cadavers were 20 females (age 57 – 98 years) (peripheral bones taken from the left side: 13, from the right: 7) and 10 males (age 60 – 94 years) (peripheral bones taken from the left side: 3, from the right: 7).

It is known that bone specimens obtained from formaldehyde-prepared cadavers contain air in the bone marrow region. The experimental set-up to extract air from the specimens was finished in March 2001. It includes an excicator, vacuum pump, manometer, and all the appropriate connectors. Formaldehyde/alcohol solution, plastic welder, and plastic bags were needed as well. The equipment and material was purchased for this project.

Establishing the air extraction procedure required experimentation and consultation with the Institute of Anatomy of the LM-University at Munich. All 180 specimens are airtight packaged and kept in a refrigerator.

## **Imaging of 180 Bone Specimens and BMD Measurements**

### **pQCT Imaging**

A Standard Operational Procedure (SOP) for BMD measurement and imaging of each skeletal region by pQCT was written. The scanning required the invention of new table fixations, a new table construction, and the invention of positioning support material.

A special configured XCT 2000 scanner providing high-resolution images was leased for a fee from Stratec Medizintechnik GmbH in Pforzheim, Germany.

All images and all BMD-measurements of all specimens from all skeletal regions were performed on this pQCT-scanner. The slice thickness was 1 mm; the  $x$ - $y$ -pixel size was set to 0.2

mm  $\times$  0.2 mm. This set-up was maintained for all bones throughout the study. The task was finished in December 2001.

### **Slice location definition**

Distal Radius: 4% of the entire radius length has been subtracted from the densest part of the distal radial joint surface. That location was used for the slice location. The individual lengths of the radii were unknown. We assumed an average length for females of 240 mm and for males of 275 mm. This location is similar to patient examinations.

Proximal tibia: 17 mm distal of the densest part of the medial joint surface. This location is in the region of a potential surgical bone harvesting site.

Lumbar vertebral body L3: center of the vertebral body in the transaxial direction.

Femoral neck: The slice was taken at the thinnest diameter of the femoral neck (center of the neck) and perpendicular to the main axis of the femoral neck.

Border between femoral neck and femoral head: A slice was taken in the area between the femoral neck and the femoral head. The rectangle to the main axis was determined on a radiograph.

Femoral head: The slice was taken transaxial at the location of the largest diameter.

Calcaneus: The slice was taken perpendicular to the anatomical length axis. The location was 20% of that length subtracted from the dorsal end.

Calcaneus: Due to the enormous geometrical variation of this bone, a second slice was taken at 30% location.

Midshaft humerus: The slice was taken perpendicular to the axis at the middle of the bone. The center was determined on a radiograph.

### **Phantom Tests Performed on pQCT**

Experiments on resolution were performed at FUB. The phantom tests showed an improved signal/noise ratio, excellent detail resolution, and very good contrast. Therefore, a noise reduction procedure as recommended by a project board meeting was not needed. In addition, the images were compared with the results of two scans acquired on a different pQCT-scanner (Densiscan) by Scanco Medical AG. The image quality obtained on the special scanner by Stratec Medizintechnik GmbH was superior. A better image quality was not obtainable on any commercial pQCT-scanner at that time.

### **BMD-Measurement of Lumbar Spines**

Exactly the same vertebral bodies were scanned on a CT-scanner Somatom Plus S in QCT-mode at FUB. This procedure was performed in two different  $x$ - $y$ -resolutions:  $0.182 \times 0.182$  mm and  $0.323 \times 0.323$  mm. The first relates to a high-resolution mode, while the latter is the resolution obtained on patient examinations. In both resolution modes, slice thicknesses of 1, 2, 4, 8, and 10 mm were obtained at the midvertebral transaxial location of the vertebral body. The lumbar spines were not moved or touched between each of the ten scans.

### **QCT of the Femoral Neck**

The initial proposal envisioned the scanning of the femoral neck on a CT-scanner. Due to a decreased market demand, the development of the QCT-software to measure the BMD of the femoral neck was stopped. It was concluded at a project board meeting that the project will not insist on QCT-scanning of the femoral neck.

## Radiography

Radiographs in two views were taken from all 30 tibiae. In addition, radiographs were taken from all 30 proximal femora in one view, from all lumbar spines in two views, from all calcanei in two views, and from all humeri in one view. The radiographs were necessary to define a repeatable slice location and for the correct positioning of the bones on the examination table of the pQCT-scanner.

All tibia biopsies were x-rayed in two views in mammography technique.

## Image Resolution and Measures of Complexity

It was found at the very beginning that the pixel size of human vertebral body images obtained from CT-scanners has an influence on measures of complexity. This influence is of a magnitude which cannot be ignored. Therefore, in preparation for 2D measurements on bones from different skeletal sites, the problem of pixel size influence on measures of complexity had to be studied, defined, and a solution to be found. Extensive experimentation in a true team effort involving all academic and industrial partners led to a conclusion in July 2001:

- ✚ Whenever possible a standardization of CT-image acquisition should be achieved when specimens or patients are scanned: zoom factor 2.2 or FOV 100.

The strict application of a standardized zoom factor or the FOV cannot be guaranteed. An alternative method to compare measures of complexity calculated from images taken at different zoom factors was needed.

An image scaling algorithm based on a Lanczos filter kernel is suitable for vertebral trabecular bone within a magnification range of 1.9 to 2.6. Using this algorithm to reach the standardized zoom factor 2.2 as a preprocessing step will lead to comparable results for magnifications differing from 2.2.

The error introduced by the resampling algorithm is below 5%, whereas non-preprocessed images with different magnifications produce non-comparable results.

An alternatively developed geometrical correction algorithm may be used in the future to detect problems with magnification factors from other skeletal regions.

## Measures of Complexity for 2D Images from Different Skeletal Locations

The technique consists of three main stages which are executed in the following order:

**1. Image preprocessing** entails a standardized segmentation of a ROI (bone) from the rest of the CT-image and splits the ROI into three data sets: entire, trabecular, and cortical bone. The technical requirements to segment the bone area from the connective or soft tissue and formaldehyde filled plastic bag have been described in detail in prior publications. However, further refinement of the algorithm to select the ROI in a vertebral body was necessary. It was accomplished in October 2001.

**2. Image encoding** simplifies the image and for every pixel it substitutes its gray-scale value by a symbol. Thereby, the level and the dynamics of the x-ray attenuation in the vicinity of the considered pixel are taken into account. This reduces the amount of gray-shades, whereas the image resolution itself is maintained. Two encoding parameters must be specified: static-dynamic threshold  $e_{ds}$ , marrow threshold  $a_m$ . For the specimen study they are set to  $e_{ds} = 80$  pQCT values,  $a_m = 275$  pQCT values.

These parameters relate to the levels and dynamics of attenuation representing the structure of the underlying materials.

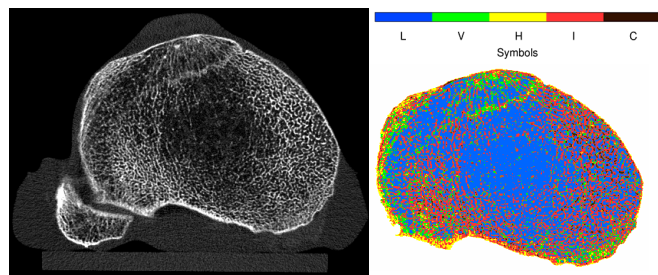


Fig. 1: Specimen 129-99; proximal tibia image as acquired (left) by pQCT, and after image preprocessing and image encoding (right). The image on the right is the prerequisite for the quantitative assessment by measures of complexity.

**3. Quantitative assessment.** The subsequent calculation of measures of complexity is based on the analysis of the preprocessed symbol-encoded images. Three data sets are available for each 2D image: entire bone, trabecular bone, and cortical bone.

Six measures of complexity can be calculated from every dataset of all skeletal locations. The measures are:

- ✚ SCI (a measure for the degree of compositional complexity),
- ✚ TNI (a measure for the intricacy of the trabecular network),
- ✚ SDI (an index about the disorder of the structural composition),
- ✚ IGE (an index for the spatial dynamics within the data set),
- ✚ Max. Size L-Block (a measure representing the replacement of hard tissue by marrow),
- ✚ Mean Size L-Block (a measure representing the average marrow size).

The calculation of complexity measures from bones of different sizes requires an appropriate width of a moving window  $N$  that collects and analyzes local statistics (block size). It has been set to be appropriate for analyzing both small and large bones. Thus, all three parameters of the numerical scheme to calculate the complexity measures ( $e_{ds}$ ,  $a_m$ ,  $N$ ) were set to their optimal values and kept constant during the evaluation of all skeletal locations.

The algorithms for computing these measures have been thoroughly tested on 2D images from all available bone regions. Additionally, they were applied to mathematical models. The outcome was very positive and encouraging. This set of parameters can

- ✚ quantify the architecture of bones from different skeletal regions,
- ✚ distinguish these skeletal regions from each other,
- ✚ quantify changes in the structure very sensitively,
- ✚ detect changes before a trained radiologist is able to detect them visually (performed on mathematical models only),
- ✚ demonstrate that structural changes are more pronounced than changes in BMD,
- ✚ identify structure even in images with an unfavorable S/N ratio,
- ✚ differentiate general structural bone loss from other localized causes.

The current set of parameters can be expanded when the need arises, or can be modified for the application of specific needs.

Since the pQCT-scanner is always calibrated before the image acquisition and the relation between the pQCT values and BMD has been found experimentally, it is possible to calculate the BMD from exactly the same area which is used for the calculation of complexity measures. This is the first time to use BMD obtained from specified ROIs. We call this parameter *calculated BMD* to distinguish it from the measured BMD which is provided by the scanner software and relates to a slightly different area of interest.

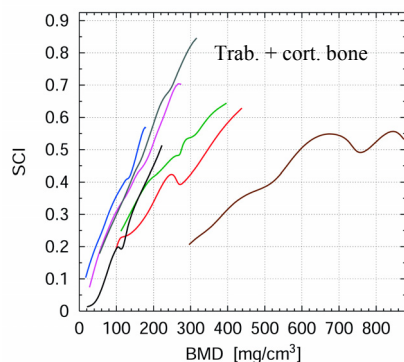


Fig. 2: Complexity measure SCI versus calculated BMD. For visualization purpose the data are approximated by Bézier curves. The curves have different slopes characterizing different rates of change of complexity for a given amount of bone loss. When evaluating a particular BMD-level, for instance  $200 \text{ mg/cm}^3$ , the respective complexity of the bone architecture differs considerably from one location to another.

Color codes: Tibia Femoral head Calcaneus (20%) L3 Femoral neck Radius Humerus

In Fig. 2 the results of the entire slice measurement (trabecular plus cortical bone) are shown. The Structure Complexity Index (SCI) shows clear differences between each bone location despite similar BMD-values. The humerus as a predominant cortical bone does not increase in complexity after it reached a BMD of about  $650 \text{ mg/cm}^3$ .

Location	Normalized slope (cort. + trab. bone)
Fem. Head	2.22
Tibia	2.17
L3	2.16
Calcaneus 20%	1.97
Fem. Neck	1.08
Radius	1.02
Humerus	0.7

Tab. 1: The value of the slope derived from normalized data is shown for each location for cortical plus trabecular bone. The data are normalized by calculating each BMD value against the highest achievable BMD of  $1.2 \text{ g/cm}^3$ ; SCI is a normalized parameter by itself. The normalized slope quantifies a relative speed of change of the structural complexity versus the BMD. Values  $>1$  mean that the complexity alters faster than the BMD. If the normalized slope is  $<1$ , the BMD changes faster than the complexity.

The conclusions drawn from Tab. 1 and Fig. 2 are:

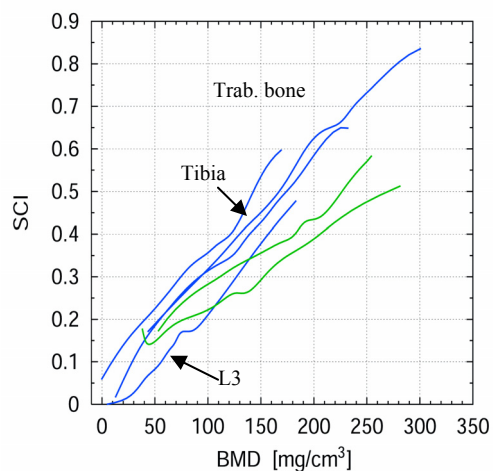
- ✚ Each region is different in its structural composition and its BMD.
- ✚ The tibia has the lowest BMD range from all bone locations.
- ✚ The steepest slope is found at the femoral head.
- ✚ Structural changes appear more rapidly than changes in BMD, except for the humerus.
- ✚ The humerus, a predominantly cortical bone, changes its BMD faster than its structural composition.
- ✚ The femoral neck and the radius as bones with a thick cortical shell behave in-between. A decrease in BMD causes less structural changes than in predominant trabecular bones.
- ✚ The highest structural complexity is found in the femoral head, the lowest in the vertebra.

The architectural complexity of cortical bone alone (humerus) does not increase after a certain bone amassment. The variation of architectural composition can saturate. A further increase is not possible, even if more material is build into it.

The radius and the femoral neck are structurally stable bones: The same amount of BMD-change produces 2 times smaller structural alterations than in the other skeletal locations with rich trabecular architecture.

Trabecular bone cannot be prudently studied by itself when we want to quantify the architecture of the bone. Even the most sophisticated cortical/trabecular separation procedure is somehow arbitrary. The cortical bone belongs to the architecture of the bone as much as the trabecular bone does. The distinction between different skeletal locales is much more pro-

nounced when we study the entire bone (Fig. 2) instead of the trabecular part of the bone only (Fig. 3).



Location	Normalized slope (trab. bone)
Tibia	2.3
L3	2.3
Fem. Head	2.28
Calcaneus	2.21
Fem. Neck	1.45
Radius	1.29

Tab. 2 and fig. 3: The value of the slope derived from normalized data is shown for trabecular bone at each location. The color represents the rate of change of SCI (normalized slope): blue denotes the bones with a fast rate, and green the bones with a smaller rate of change.

However, we can conclude from the analysis of SCI of the trabecular bone alone that

- ✚ The femoral neck and the radius behave even in their trabecular parts differently than the other predominant trabecular bones.
- ✚ The tibia has the lowest trabecular BMD, however, very similar to the vertebral body L3.
- ✚ The most sensitive trabecular parts are found in the tibia and the vertebral body. Nevertheless, the femoral head and the calcaneus behave almost similar to the tibia and the vertebral body.

The trabecular bone distinguishes two groups of location with different behavior as measured by SDI. The trabecular bone of the tibia, vertebra, and the calcaneus demonstrate an increased degree of order during bone loss, whereas the radius, femoral neck, and the femoral head show an increased degree of disorder.

The similarity in trabecular bone behavior at different skeletal locations is expressed by TNI. Despite different initial values, the rate of TNI decay is similar in different locations during bone loss.

Maximal L-block and Mean L-block reveal also similarity in response to decreased BMD at different skeletal locations: connected areas of soft elements (marrow) grow in size exponentially with the maximal rate of change found in bones with lowest BMD.

IGE evaluates the dynamics of assembly of structural elements which varies greatly depending on the skeletal region, despite the same BMD. IGE demonstrates that although the femoral head and femoral neck are less than 5 cm apart from each other and might have the same BMD, the difference in architectural composition is dramatic. The IGE of the femoral head is two times higher at a BMD=100 mg/cm<sup>3</sup>, and for BMD=300 mg/cm<sup>3</sup> it is three times higher than the IGE calculated from the femoral neck (see Fig. 4).

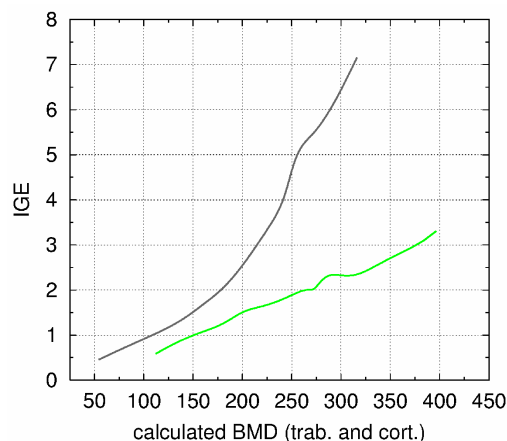


Fig. 4: Complexity measure IGE versus calculated BMD. The two curves represent the femoral head and the femoral neck. Although the distance between the two locations is about 5 cm, the architectural composition is very different. Both skeletal regions are structurally configured to be exposed to different loading conditions. This structural difference is being expressed quantitatively with the structural measure of complexity IGE.

The reference bones for bone density measurement are the lumbar vertebral bodies. We found that the proximal tibia is similar in its BMD value and in its architectural composition. Since the proximal tibia is easier to reach, has less soft tissue around it and, therefore, has a higher S/N ratio in radiological imaging. In patient measurements, its smaller volume produces images with much higher resolutions. It might be the better location for quantitative assessment of the bone status than the lumbar vertebrae.

The sensitivity of architectural changes is the highest in the trabecular bone of the tibia and, similar, in the lumbar vertebral body. If the cortical bone is included in the calculation of the bone status, the tibia is slightly the better bone for the quantification procedure.

Bones with large amounts of cortical bone surrounding the trabecular part of the bone, such as the radius and the femoral neck, have a much lesser sensitivity to changes in their composition. Therefore, the radius as well as the femoral neck is not an ideal location for a bone status evaluation.

The Spearman's Rank-Order correlation coefficient  $R_s$  was calculated between different skeletal sites using the BMD and the measures of complexity. The strongest correlation is found between the bones of the same upper (humerus, radius,  $R_s \geq 0.64$ ) and lower (calcaneus, tibia, and femoral head,  $R_s \geq 0.82$ ) extremities. The biomechanical induced architecture behaves very similar in the bones of the same side extremity. The lowest correlation ( $R_s < 0.36$  for the SCI, and  $R_s < 0.58$  for the BMD) is found between the vertebra and peripheral bones. This is an indication that the structure of the axial skeleton differs from the peripheral bones.

Intrapersonal, the highest structural complexity is found in the femoral head, the lowest in the vertebra.

In general, the correlation between all skeletal sites of the whole (cortical + trabecular) bone is stronger ( $R_s = 0.49 \div 0.9$ ) than in the trabecular bone alone ( $R_s = 0.38 \div 0.86$ ). This confirms our suggestion that the whole bone needs to be evaluated for quantification, rather than the trabecular bone alone.

## Bone Modeling

2D simulations were performed as numerical experiments. These utilized a regular lattice to simulate trabecular bone tissue, and later CT-images of human vertebral trabecular bone tissue. The results were important for further development of the measures of complexity. We came to the following conclusions:

- ✚ Measures of complexity are very sensitive in the detection of local defects and local elements which appear invisible to the eye.
- ✚ Measures of complexity are very sensitive to the appearance of disorder, and are equally good in the detection of order or disorder.
- ✚ Measures of complexity can differentiate between regular or random changes.
- ✚ Measures of complexity are more efficient than BMD-measurement concerning the description of changes in a given bone slice.

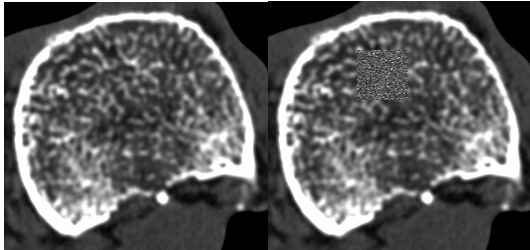


Fig. 5: Example of 2D numerical experiments. Left: CT-image of a human L3 vertebra in its original form. Right: Same CT-image with a little window in which the 15. iteration of random remodeling is visualized.

The BMD is kept constant but the change of structure is visible. The 2D measures of complexity are very sensitive to changes like this.

A 3D model was essential because the 3D data sets obtained by  $\mu$ -CT demanded adequate mathematical explanations. The model simulates the bone deterioration by the activation of the basic multicellular unit (BMU) in randomly chosen locations on the bone surface, resorption of the bone material, and the termination of its activity after some random time. The modeling process helps in the interpretation and is able to extrapolate the data curves beyond their ends which were given by the random sample we collected from the Anatomical Institutes.

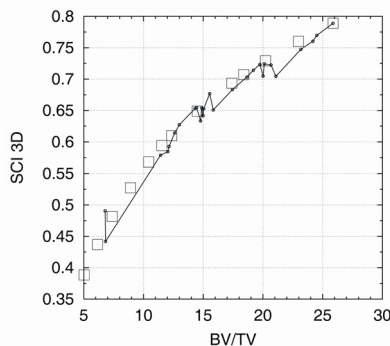


Fig. 6: Example of 3D modeling. BV/TV results from a 1cm long VOI of a tibia bone biopsy versus a 3D measure of complexity (SCI 3D). The black line represents real data obtained by  $\mu$ -CT from 27 biopsies. The squares are data from a 3D bone model.

Although the model had been formulated before the real data became available, the real data fit the estimations very well.

## Acquiring Bone Biopsies from Human Tibiae Specimens

In order to verify the changes in structural composition measured on 2D images, the quantification of 3D data sets from the same skeletal region is essential. The 3D data sets can be derived from bone biopsies which were scanned by  $\mu$ -CT. It was proposed to use tibia bone biopsies as a most accessible site for harvesting trabecular bone.

The biopsies were taken at the medial side 17 mm distal of the tibia plateau. This location is a surgical site for harvesting trabecular bone grafts.

All 30 biopsies have a diameter of 7 mm. The length of the biopsies varies between 2 and 4 cm. There were 3 biopsies which provided biopsy cylinders of 1 cm length only.

## Preparation of the Tibia Biopsies for $\mu$ -CT Scanning

All 30 tibia biopsies were embedded in methylmetacrylate. Due to problems regarding the hardening of the embedding material, the procedure needed some adjustments. A new im-

proved procedure was experimentally found. The biopsies were embedded in 14 mm wide cylinders. This preparation allowed easy shipment between the academic and industrial partners. As proposed, the biopsies were scanned at the  $\mu$ -CT at FUB and at Scanco Medical in Zurich, Switzerland.

### 3D Scanning of Tibia Biopsies

Calibration issues of the  $\mu$ -CT scanners were tried to solve at FUB before the tibia biopsies were scanned. The appropriate voxel size is 32  $\mu\text{m}$  for the size of the biopsy cylinder at FUB's  $\mu$ -CT. Most of the biopsies needed to be scanned in two sessions, due to their length. ZIB developed a program to stack the parts on top of each other. There is no loss of data information in that process.

The voxel size is 20  $\mu\text{m}$  for the biopsy cylinders at Scanco's  $\mu$ -CT. Although the trabecular network appeared to be the same in both data sets, the details of their appearance (edge definition, internal trabecular attenuation, and machine related artifacts) were different.

Therefore, other  $\mu$ -CT users and manufacturers were contacted and asked to scan a maximum of 3 of our biopsies. We collected results from BAM (Bundesanstalt für Materialforschung (Berlin) [ $\mu$ -CT and Synchrotron], Skyscan (Netherlands), and EVS (Canada); while the  $\mu$ -CT scanner at FUB was upgraded (three different versions).

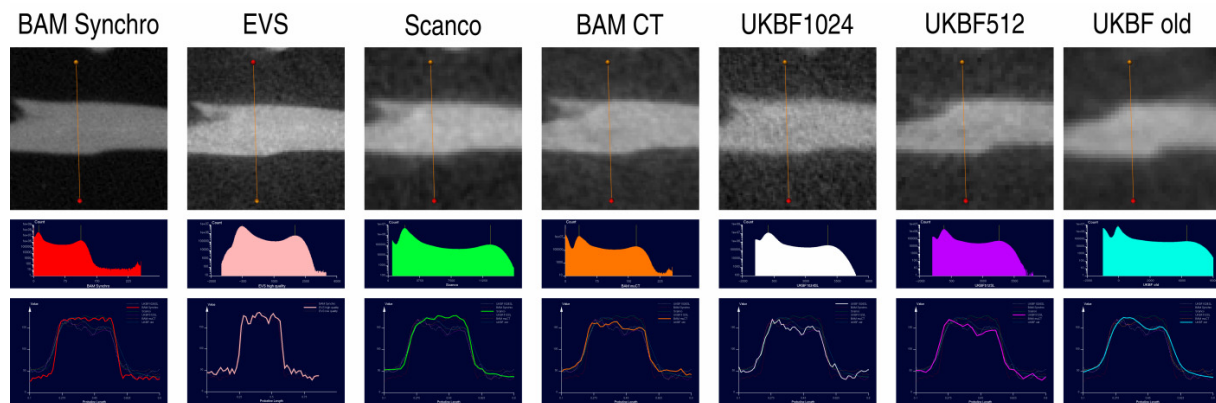


Fig. 7: Comparison of image quality of one trabecula obtained from sample 87-99 at different  $\mu$ -CT scanners. The first row is the visualization of a small part of a trabecula, the second row is the probability distribution of the X-ray attenuation from the entire biopsy, and the third row is the grey value profile through the trabecula along the orange line shown in the first row. BAM Synchro = Synchrotron image, EVS =  $\mu$ -CT scanner from EVS, Scanco =  $\mu$ -CT scanner from Scanco Medical AG, BAM CT =  $\mu$ -CT scanner from BAM, UKBF1024 =  $\mu$ -CT at FUB with upgraded 1024 matrix, UKBF512 =  $\mu$ -CT at FUB with upgraded 512 matrix, UKBF old =  $\mu$ -CT at FUB before upgrading.

The best image quality results from synchrotron imaging, followed by the  $\mu$ -CT from EVS. The  $\mu$ -CT scanner from Scanco provided better quality than what was achievable at FUB. The image of Skyscan's  $\mu$ -CT is not shown due to its inferior image quality. The synchrotron as well as the  $\mu$ -CT system by EVS is not available for this project, therefore, the decision was made to use the data sets obtained at Scanco for further analysis and for the development of the 3D measures of complexity.

### Damage Assessment and Identification of Potential Artifacts in Biopsies

The manual procedure to acquire biopsies from human bones has a high potential for artifacts that would influence the appearance of the trabeculae within the biopsy, and therefore, would

have effects on any type of quantification as well. We decided against the manual procedure in April 2001 after preliminary experiments showed the potential hazards.

In cooperation with the Dept. of Trauma Surgery at FUB, a bone-safe procedure requiring an AO surgical drill performed under fluoroscopic conditions was established. The biopsies were acquired with a diamond coring drill. The utmost care and the best possible precision were taken for the procedure. Visual inspections of the bone biopsies led to the conclusion that the material is completely intact. The  $\mu$ -CT scans of the first biopsies confirmed our visual observation that there was no damage to the trabeculae. However, we found bone dust, due to the cutting diamonds inside the coring drill, in the outer parts of the biopsies. These bone particles are very small (max. 2  $\mu$ m). They are located in the soft tissue between the trabeculae and around the entire circumference of the biopsies. The dust particles reach as deep as 0.7 mm into the probes. The drilling residue is easily identifiable and the standard method for removal of drilling residues in bone histomorphometry is to edit these particles with image editing software. Whereas in  $\mu$ -CT studies, the standard for removal of drilling residue is to consider only a sub-area of the volume by excluding a small zone of bone tissue that is nearest to the edge of the biopsy. Both methods for removal of the drilling residues are valid and widely used.

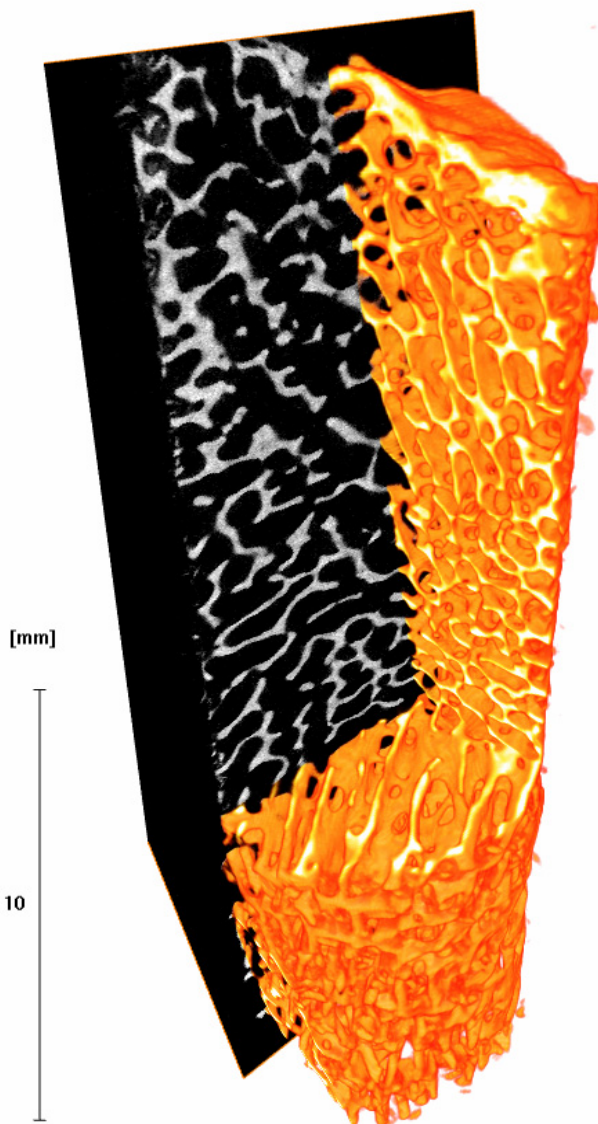


Fig. 8: Example of a visualization of parts of a 3D bone biopsy data set derived from  $\mu$ -CT by Amira. The background shows the coronal 2D view in black and white. The orange colored trabecular network is cut in the lower part to demonstrate an axial view, and cut at the right to show a sagittal view of the trabecular bone.

At the edge of the biopsy in the frontal view (left side) the small bone dust particles are seen within the marrow space between the trabeculae.

(The anatomical directions are mentioned according to the bone tissue direction within the proximal tibia.)

Animations of 3D data sets from human tibia biopsies are shown on our website <http://bone3D.zib.de>

ZIB developed within the Amira framework a procedure to determine and to select a defined VOI within the volume of the biopsy.

It was found that it is not possible to make all bone sections acquired by  $\mu$ -CT and histomorphometry 100% identical. During sectioning of the histological samples, the knife of the microtome will stretch the very thin (10  $\mu\text{m}$ ) embedded sections in the direction parallel to the microtome knife. This stretching may not even be uniform over the length of the section. During the mounting of the thin sections onto microscope slides, there is a possibility of creating wrinkles in the sections and there is a risk for the sections to be damaged. As a consequence not all of the histological sections are of a high quality necessary for comparison with the  $\mu$ -CT sections.

In order to perform histomorphometry, the sections must be segmented into bone and marrow. This is carried out through a threshold filtering process. For technical reasons of different gray-scales in histomorphometry and  $\mu$ -CT, it is not possible to use exactly the same level for the threshold filtering in the histological samples and the  $\mu$ -CT sections.

The cutting direction of the biopsies was decided in conjunction with consultations of Prof. Parfitt (USA) and Dr. Amling (Germany). The cuts were made in the frontal loading direction of the trabeculae.

For the purpose of this project the damage assessment of bone biopsies revealed no damage when biopsies were taken with power-driven surgical coring drills, other artifacts were investigated and solutions were found. The method described here can be used for bone biopsy attainment in patients or space-flying personnel.

### **Quantification of the Trabecular Bone Structure with Traditional 2D Histomorphometry – Relationship to 3D $\mu$ -CT evaluation**

The embedded and  $\mu$ -CT scanned tibia biopsies were further embedded in Technovit 3040 (Heraeus Kulzer, Wertheim/Ts, Germany) so that the cylindrical shaped embedded bone samples could be fixated in a microtome. The samples were cut in 10  $\mu\text{m}$ -thick frontal sections on a Jung model K microtome (R. Jung GmbH, Heidelberg, Germany). The cuts were taken from the central 2 mm of each biopsy. Two 10  $\mu\text{m}$ -thick sections separated by 10  $\mu\text{m}$  formed a disector pair. Six consecutive sections were cut, stained, and mounted and, from these four possible disector pairs, the pair with the fewest sectioning artifacts was selected for further analysis. The distance between two sets of six consecutive sections was 180  $\mu\text{m}$ . All sections were stained with aniline blue (modified Masson trichrome). The mounted 10  $\mu\text{m}$ -thick aniline blue-stained sections were placed in an Agfa Arcus II image scanner (Agfa-Gevaert AG, Leverkusen, Germany) with an integrated transparency scanning unit. Digital images of the sections were acquired with Agfa Fotolook 2.09 (Agfa-Gevaert AG) in the “line art” setting (1 bit images) at a resolution of 2.540 dpi (pixel size: 10  $\mu\text{m} \times 10 \mu\text{m}$ ). The threshold during image scanning was determined by scanning one bone section at different thresholds and selecting the threshold that gave the closest resemblance of the digitized image of the bone section by visual inspection. The GNU Image Manipulation Program (GIMP) (<http://www.gimp.org>), running under the Linux operating system (Red Hat Linux 6.2, Red Hat Software, Inc., Raleigh, NC) was used to remove artifacts from the images. During the removal of artifacts, comparison was made between the computerized image and the section using a stereo microscope (Olympus SZ-40, Olympus, Tokyo, Japan). In order to make the comparison between the 2D histological sections and the 3D  $\mu$ -CT data sets as realistic as possible the drilling resi-

due was left in place in the 2D histological sections. However, the drilling residue was excluded from the ROIs in both the 2D and 3D analyses.

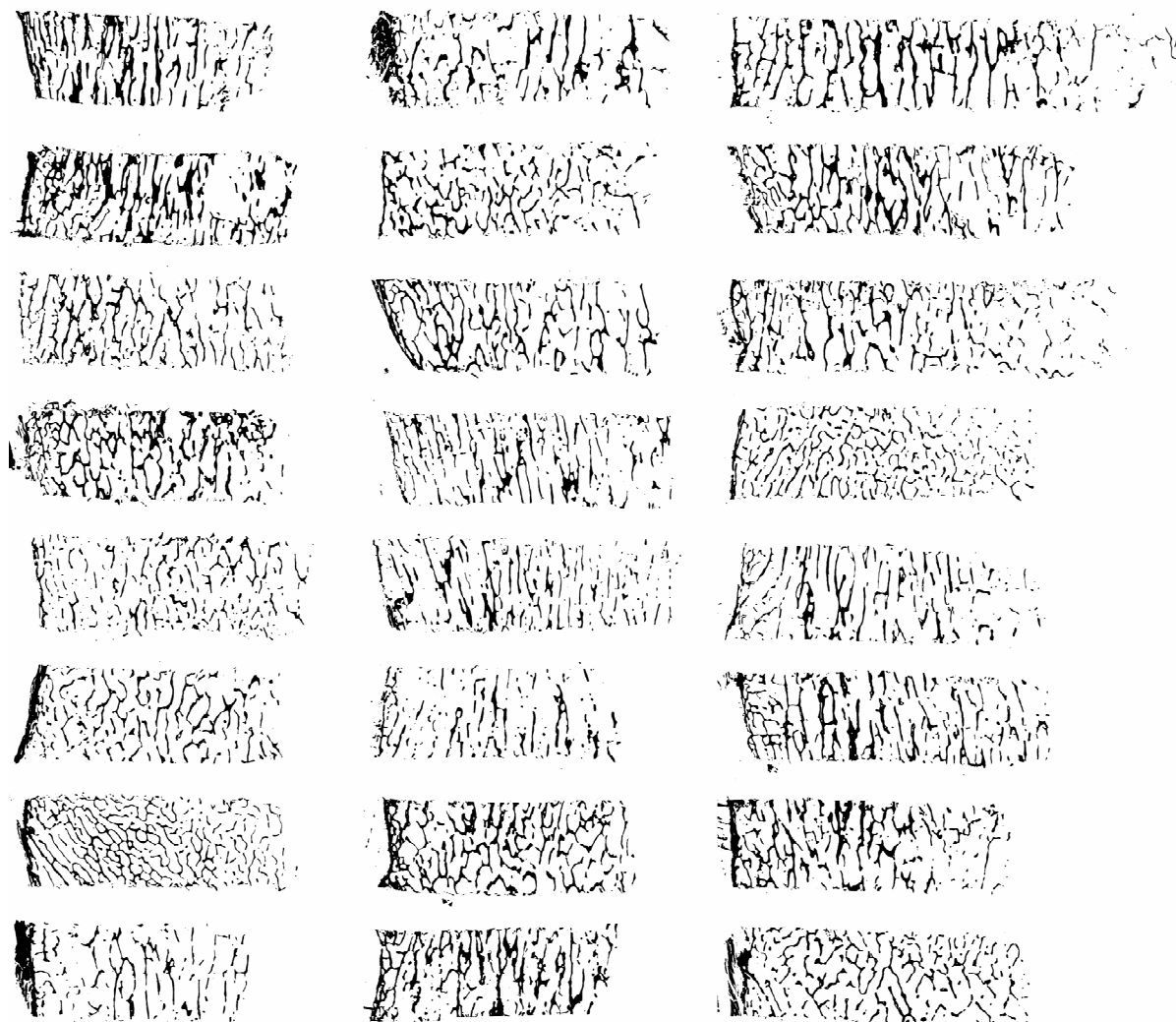


Fig. 9: Example section from each of the biopsies. Notice the differences in length and how the structure changes even within a biopsy. The structural composition thins out in relation to the distance away from the cortical shell (left on each biopsy).

The trabecular bone structure and trabecular bone volume is not constant through the entire length of the biopsies (Figs. 9 and 10). Consequently, it was decided that all sections should be analyzed with two ROIs: One covering the whole biopsy and the other covering a 1-cm-long zone placed 0.5 cm below the cortical shell (Fig. 10). The latter ROI was experimentally found as the region with the most stable BV/TV.

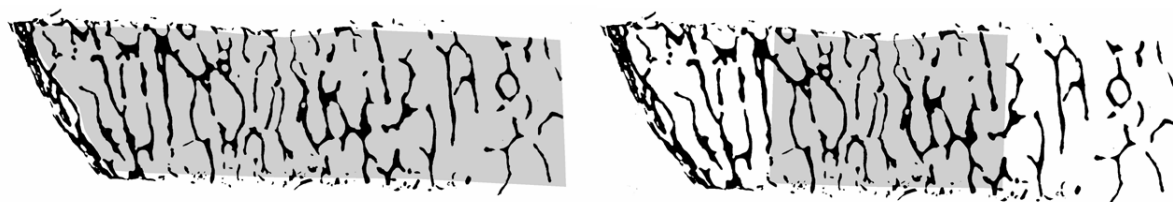


Fig. 10: Example of a histological section. Both the full ROI and the 1 cm long ROI are shown.

The following standard histomorphometric measures were determined for both ROIs:

- ⊕ trabecular bone volume (BV/TV)
- ⊕ marrow and bone space star volume
- ⊕ trabecular thickness (Tb.Th)
- ⊕ trabecular number (Tb.N)
- ⊕ trabecular separation (Tb.Sp)
- ⊕ node-terminus ratio (Nd/Tm)
- ⊕ trabecular bone pattern factor (TBPf)
- ⊕ connectivity density (CD).

BV/TV and CD are the most important histomorphometric measures: BV/TV quantifies the amount of bone material present, whereas CD is a parameter to quantify a certain aspect of the structure of the trabecular network. The connectivity density expresses the number of times the network branches minus the number of free ending trabeculae per tissue volume. The connectivity density can be defined in exact mathematical terms from Betti numbers or Euler numbers, both are well defined topological properties of the trabecular network [1]. In order to determine the connectivity density using normal histological sections, the so-called ConEulor method was used [2].

Trabecular thickness, trabecular number, and trabecular separation were calculated using the parallel-plate model. From measurements of bone area (B.Ar), marrow area (Ma.Ar), tissue area (T.Ar), and the length of the bone marrow interface (B.Pm); the parallel-plate model of Parfitt et al. calculates thickness and separation of the bone tissue, assuming the tissue is equally distributed as parallel plates. Tb.Th is the thickness of the plates, Tb.N is the number of plates per unit length, and Tb.Sp is the separation between the plates. In 3D, B.Pm is replaced with the area of the bone surface. The B.Ar and the T.Ar are replaced with the corresponding volumes.

The correlation between the length of the bone marrow perimeter and the bone surface area may be dependent on the shape of the trabeculae being mostly rod-like or mostly plate-like. The parallel-plate model involves the determination of the length of the bone marrow perimeter in 2D, whereas it involves the determination of the bone surface area in 3D. Since the ratio of rod-like trabeculae to plate-like trabeculae is different for each biopsy, it will weaken the correlation between the measurements performed in 2D and in 3D.

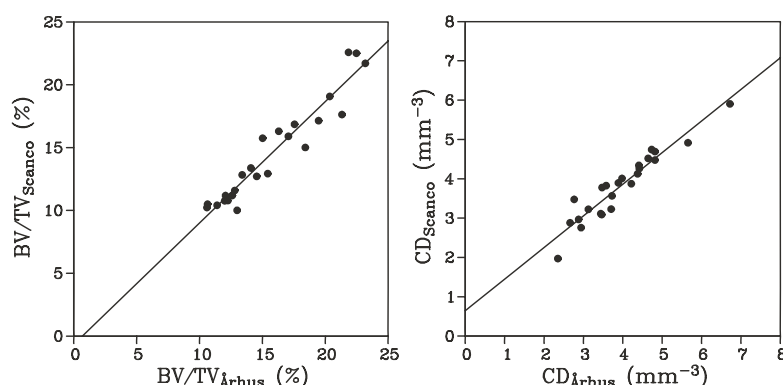


Fig. 11: Comparison between BV/TV and CD measured by histomorphometry (UoA) and by  $\mu$ -CT (Scanco). Refer to Tab. 3 for correlation coefficients. For BV/TV, neither the slope nor the y-axis intercept are significantly different from 1 and 0 respectively. For CD, the slope is significantly ( $p=0.0024$ ) different from 1 and the y-axis intercept is significantly ( $p=0.011$ ) different from 0.

Using the 3D data set obtained by  $\mu$ -CT, Scanco determined BV/TV; Tb.Th; Tb.N; Tb.Sp; and CD for the full ROI only. The histomorphometric measures obtained by histomorphometry (UoA) and by  $\mu$ -CT (Scanco) were compared using data for the ROI covering the whole biopsy (Fig. 11).

	$r$	$p$
BV/TV	0.96	$2.11 \times 10^{-13}$
Tb.Th	0.79	$5.26 \times 10^{-6}$
Tb.N	0.74	$4.27 \times 10^{-5}$
Tb.SP	0.89	$1.16 \times 10^{-7}$
CD	0.95	$1.66 \times 10^{-12}$

Tab. 3: Correlation coefficients and level of significance for the relationships between 2D and 3D histomorphometric measures.

The comparison between the 2D and 3D data results in excellent correlations (Tab. 3). The two most important histomorphometric measures BV/TV and CD show the strongest correlations. Strong correlations are also seen between the parallel plate model parameters even if these correlations are weaker than those for BV/TV and CD. These tight correlations between the 2D and 3D measures are an indication that the work was performed with utmost care, even if the sectioning caused artifacts. Preparation, artifact repair, and cutting direction are other probable reasons for errors.

However, the very strong correlations are striking when it is considered that the 3D measures are based on data from the entire diameter of the biopsies, whereas the 2D measures are based on 16 10- $\mu$ m-thick sections only.

The reason why the correlations are weaker for the parallel plate model is probably that this method is more difficult to extend from 2D to 3D (as mentioned above) than the determination of BV/TV and CD. We are now able to compare directly histomorphometric measures (gold standard) with new 3D measures of complexity derived from  $\mu$ -CT data sets.

References for this chapter:

1. Odgaard, A. and Gundersen, H. J. G.: Quantification of connectivity in cancellous bone, with special emphasis on 3-D reconstructions. *Bone* 14; 1993: 173-182
2. Gundersen, H. J. G., Boyce, R. W., Nyengaard, J. R., and Odgaard, A.: The ConnEulor: Unbiased estimation of connectivity using physical disectors under projection. *Bone* 14; 1993: 217-222

### **Appropriateness to Use $\mu$ -CT Data Sets for 3D Measurements of Complexity**

In order to investigate the usefulness of  $\mu$ -CT data sets for 3D measurements of complexity, ways of how to transfer our ideas of 2D complexity measurements into the 3D space, and how to deal with large amounts of data were investigated.

The German academic partners achieved a workable transfer of symbolic dynamics and symbol-encoding from 2D to 3D. The investigations about the edge definition and the attenuation distribution in the trabeculae led to the conclusion that the five-symbol-encoding method is too sensitive for  $\mu$ -CT data. It may be useful for synchrotron-based data sets. However, a reduction to 3 symbols (for marrow, bone surface [one voxel thick], and bone) resulted in a successful transfer of symbolic dynamics to 3D.

Another way to develop 3D measurements of complexity was a reduction of the amount of data to its essential structural geometry. ZIB developed a method of skeletonization of the trabecular network. Together with the local thickness, which can be color-coded on the surface, the original information is still kept within the reduced data set.

The 3D data sets obtained by Scanco  $\mu$ -CT scanners are appropriate to be used for the invention and development of 3D measures of complexity. The edge definition of the data obtained with the  $\mu$ -CT scanner at FUB is not precise enough to differentiate a one-voxel bone surface from the bone itself.

### Skeletonization of the Trabecular Network and Other Visualization Tools as a Basis for Structural Quantification

The visualization software, the Amira platform, has been further developed. One direction is the improvement of the visualization of large 3D data sets. The other direction is the development and incorporation of quantification tools. Both objectives are essential for this project.

A skeletonization method reduces the trabeculae to a central plane. This plane is one voxel thick. In order to preserve the local thickness of the trabeculae, the skeleton received a continuous color code. This method is work in progress and will be further developed during the second phase.

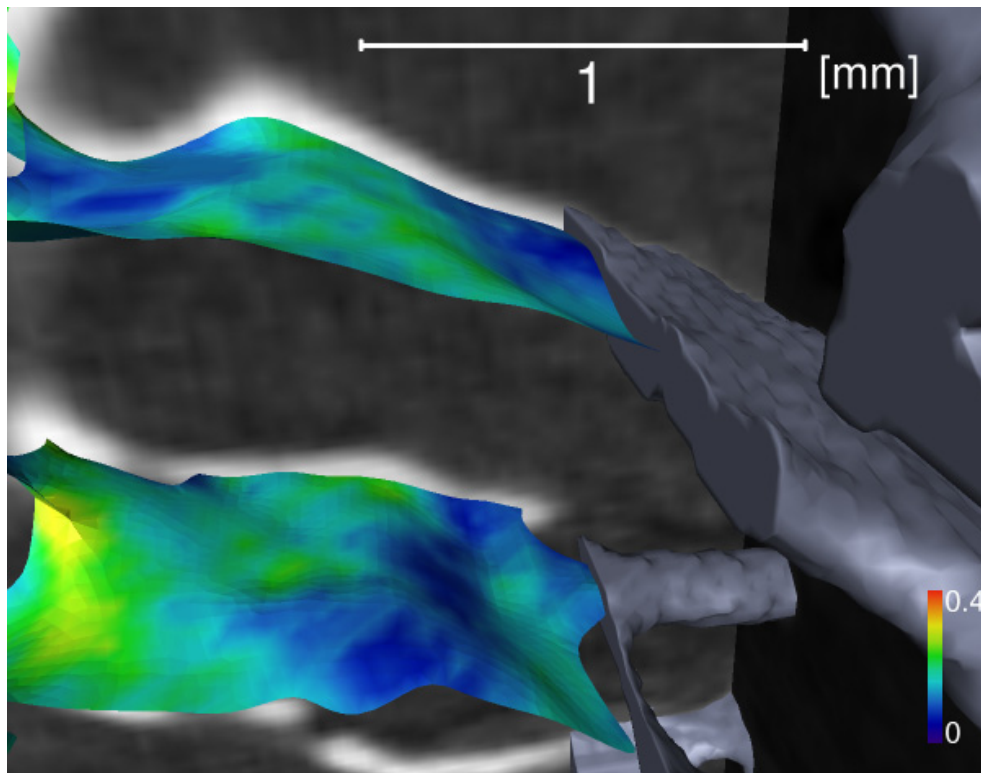


Fig. 12: Detail of a color-coded skeletonization in comparison with 2D (background) and 3D reconstructions (right) of a tibia bone biopsy. The skeleton itself is located in the geometrical center of the trabeculae. This can be seen at the border to a 2D sagittal plane on the left, and on the right in comparison to a 3D coronal reconstruction. Color and length scales are provided.

The visualization algorithms and its additional tools are constantly improved by ZIB and developed further. Improvements specific to the project are:

- ✚ changes in the resampling module for investigating resampling artifacts,
- ✚ special import function for the  $\mu$ -CT data,
- ✚ modules to handle data sets that do not fit into main memory,
- ✚ module for merging several blocks to one large data set with seamless transitions,
- ✚ histogram module that allows to restrict the calculation to a VOI,
- ✚ development for modules to calculate 3D measures of complexity.

- ✚ General improvements in Amira (by ZIB and its spin-off Indeed – Visual Concepts) that are relevant for the project:
  - ⊕ Improvements in the calculation of distance maps.
  - ⊕ New features for interactive image segmentation. Useful for selecting VOIs.
  - ⊕ Improvements and new tools for geometrical measurement (lengths and angles).
  - ⊕ Slice aligner: new tool for manual and automatic alignment of 2D slices in a 3D image stack.
  - ⊕ New options for resampling: specify voxel size of output data set; take dimensions and/or resolution of output from reference object.
  - ⊕ New module ApplyTransform (resamples transformed 3D image onto new grid with identity transformation, resamples 3D image onto a new grid oriented as defined by a slicing module).
  - ⊕ Volume rendering: support for palette textures and SGI/HP color table extension, real-time selection of subvolumes via a tabbox dragger.
  - ⊕ Better support for transparencies in slicing modules such as OrthoSlice and ObliqueSlice by use of OpenGL's alpha test function.

### Measures of Complexity to Quantify the 3D Structure of Bone

Before any of the proposed measures of complexity for 3D data sets were applied to the whole set of biopsies, standardization procedures had to be created.

As it can be seen in Fig. 9, the structural information varies greatly depending on the location within a biopsy. It can be appreciated as well in 3D where it may appear even more pronounced, see Fig. 13).

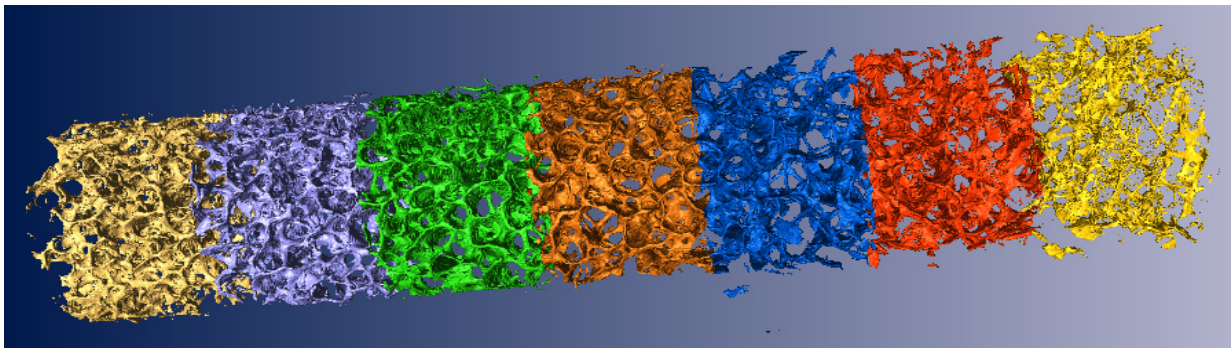


Fig. 13: Example of a human tibia biopsy split into 5 mm long fragments starting below the cortical bone (at the left). Each segment was quantified by the proposed measures providing the dependence on the position. Note the difference in structure of the first (left, directly underneath the cortical shell which was cut off for this experiment) and the last segment.

We found that within the length of 2.5 cm the measures, including BV/TV, change in an interval of 31-82%. Thus, the need for a standardized VOI arose: not only a volume, but also the position of an analyzed part must be fixed in order to produce comparable results. We concluded to use a VOI of 1 cm length where the upper edge is located 5 mm below the cortical bone. Such a VOI can be identified in the 3D data (light blue in Fig. 13) as well as in the 2D sections for histomorphometry (Fig. 10, right).

A 2 mm shift of the VOI in the direction towards the cortical bone results in changes of the structural measures less than 3%, whereas a shift in the opposite direction would produce errors > 6%.

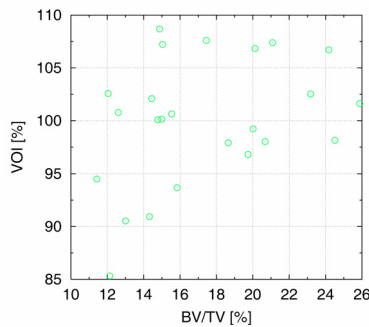


Fig. 14: An important issue has been the standardization of VOI-size and location within the biopsy. Shown is the BV/TV distribution of the sample size in comparison with the VOI. The average VOI is 366.4 +/- 22.05 mm<sup>3</sup>. The average variation from 366.4 (=100%) is +/- 6%. This is an indication that the volume is large enough to be a reliable size for the entire sample, and stable enough to produce precise results of any further quantification parameter. 1 cm high fragments of the biopsies taken at the same location within each sample provide VOIs which are a standardized representation of each biopsy.

Another important issue had been the transformation of the symbol-encoding process as applied to 2D image quantification to the 3D data sets.

Symbol-encoding preserves the robust and crucial information about the original structure but dramatically decreases the amount of information to be processed to quantify its structural organization. Unfortunately, the edge definition of the 3D  $\mu$ -CT data sets did not provide the expected clear transition between bone and bone marrow. Therefore, the idea to use a similar encoding procedure as for the 2D images was revised. Instead of the five symbols used in 2D image quantification three symbols representing the bone, the bone marrow, and the boundary-voxel between these two tissues: the bone surface.

The following measures of complexity for 3D bone biopsies are the most relevant measures among several others which were developed:

- ✚ Normalized entropy of the geometrical location of bone tissue,
- ✚ SCI3D,
- ✚ Surface Complexity Index (SurfCI),
- ✚ Surface IGE (SurfIGE),
- ✚ SCI of the BV/TV distribution (SCI(BV/TV)).

These measures quantify architectural composition in a 3D data set.

The algorithm for calculation of each measure has been designed and implemented in Amira. In addition to the proposed measures of complexity, an algorithm to calculate the BV/TV ratio directly from a given VOI of a biopsy has been developed.

Since this is work in process, other measures based on skeletonized data, and measures based on aggregation of marrow or bone volume by spatial region growing utilizing a series of spherical brushes of different radii will be released in 2003.

The results of the 3D evaluation show that the complexity of the bone structure decreases while bone mass is lost. This correlation is confirmed by two independent approaches: entropy of geometrical locations as well as symbol-based SCI3D (Fig. 15). BV/TV as a volumetric measure is correlated with trabecular BMD at 0.88.

Another interesting finding has been that the BV/TV derived from the 3D data sets is correlated by 0.96 with the BV/TV found in the histomorphometric evaluations of the 2D biopsy sections. Therefore, at least for the purpose of this project, there is no need to differentiate between 2D and 3D derived BV/TV.

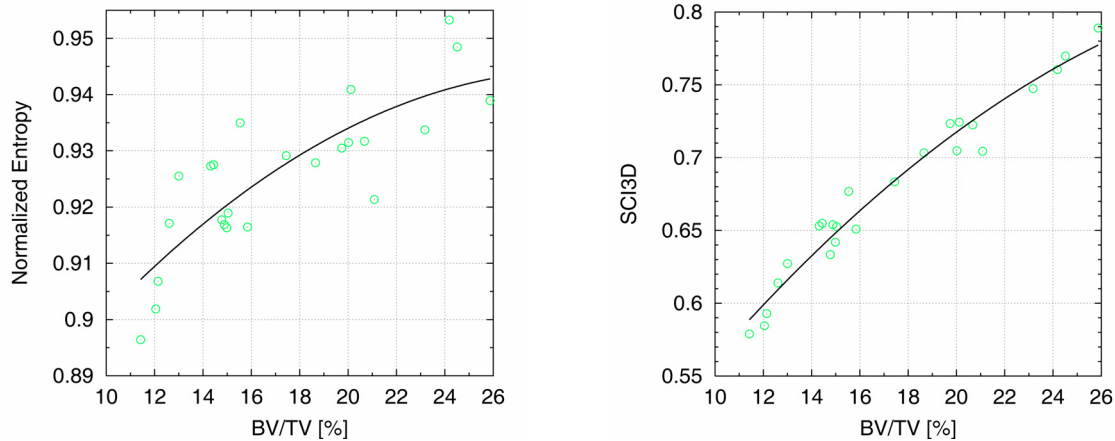


Fig. 15: Normalized entropy of the bone tissue derived from bone voxels versus BV/TV (left) and SCI3D, a structural parameter measuring the local complexity of the architectural composition, versus BV/TV (right). Both independent parameters confirm a decreasing complexity of architectural composition when BV/TV decreases.

It is also found that beyond a certain amount of bone material loss, the relative probabilities of symbols representing the internal bone voxels and the surface voxels decrease at different rates, thus capturing the difference in bone architecture.

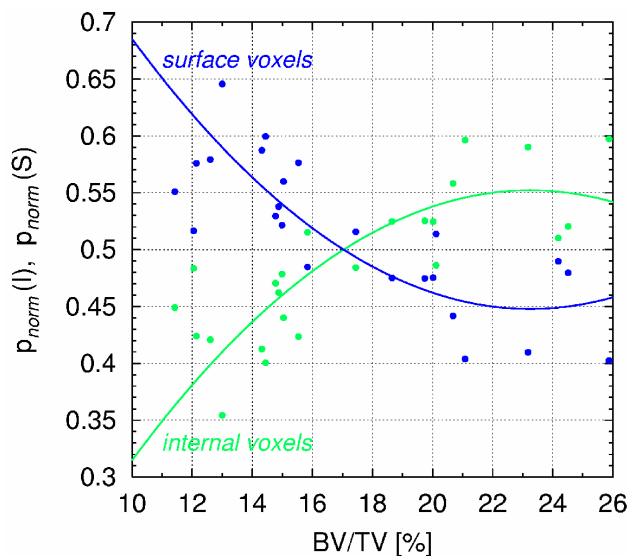


Fig. 16: This diagram shows the probabilities of the bone surface voxels and the internal bone voxels (normalized by the total number of bone voxels) against BV/TV. Relative to each other, the number of surface voxels increases, while the internal bone voxels decrease.

Fig. 16 demonstrates clearly that the relative surface of bone tissue increases when the trabeculae themselves get thinner. This happens while the amount of bone material decreases. Assuming that the osteoclasts absorb bone tissue from its surface, it means that these cells have a larger area to attack. Therefore, we do see an exponential decrease in trabecular material (internal voxels) in Fig. 16. There seems to be a switching point around BV/TV 17%, which may be a point of no return for the bone tissue to regain structural competence. This relates to an equivalent QCT-derived BMD of about 80 – 100 mg/cm<sup>3</sup>.

The findings shown in Fig. 16 were used to develop a new measure, the relative ratio between the volume occupied by bone surface voxels and the total bone volume. Since this measure represents the IGE of the surface by the given three symbols, we call it Surface Index of Global Ensemble (SurfIGE). Fig. 17 confirms the finding that an increasing BV/TV leads to a

decreasing surface relative to the internal gain of bone tissue. The trabeculae get thicker and the surface occupies less space.

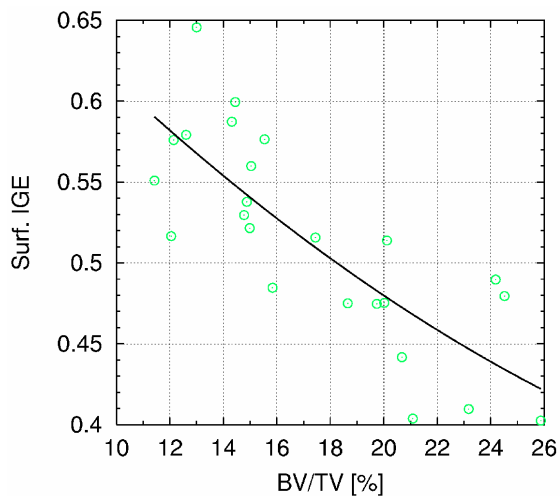


Fig. 17: The measure of complexity SurfIGE decreases when the amount of bone (BV/TV) increases. This confirms the result shown in figure 16.

By looking at the entropy of the distribution of relative local bone surface probabilities in a 3D volume, the curve in the diagram is reversed in comparison to Fig. 17. The Surface Complexity Index (SurfCI) increases when BV/TV increases. This is a definite sign that the compositional shape of the trabeculae is more complex in healthy bones.

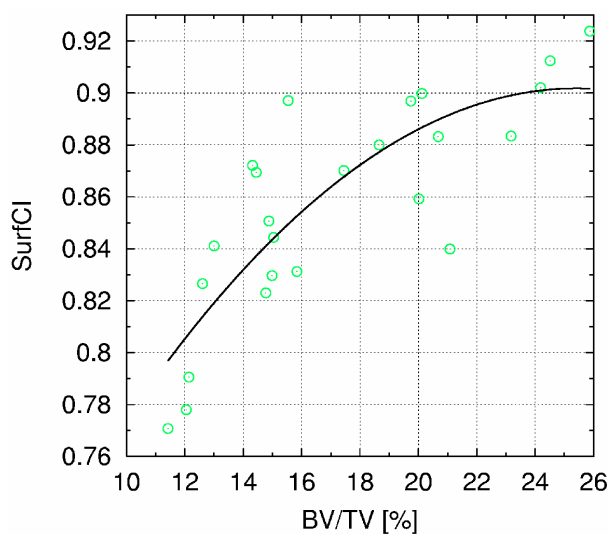


Fig. 18: Relationship between BV/TV and Surface Complexity Index (SurfCI). The complexity of the composition of the trabeculae increases with the amount of material accumulated in the bone tissue. It is also an indication that the compositional homogeneity decreases.

This Surface Complexity Index provides new information. It is well correlated with

- ✚ measures related to the amount of material
  - ⊕ BMD (0.823),
  - ⊕ BV/TV 2D (0.82), BV/TV 3D (0.795);
- ✚ with measures of construction
  - ⊕ Tb.N (0.662),
  - ⊕ TB.Sp (-0.763),
  - ⊕ Marrow star volume (-0.614);
- ✚ with measures of the distribution of the material within the tissue
  - ⊕ normalized entropy (0.945),
  - ⊕ IGE3D (0.795);
- ✚ and with measure of the complexity of the material distribution
  - ⊕ SCI3D (0.913).

This proves the importance to look for measures which quantify bone tissue in a holistic, nonlinear manner. The SurfCI is such measure. As the curve in Fig. 18 suggests already, it is expected to reach saturation with increasing BV/TV. The nonlinear behavior of natural materials suggest a decline after a saturation plateau. The decline would result in the pathologic appearance of osteopetrosis.

A biomechanical parameter derived from 2D imaging, bone strength index (BSI) has been calculated while the tibia bone samples were scanned by pQCT. The BSI is an indicator of strength; it is derived from the polar resistance moment of inertia. This parameter has surprising good correlations with all 3D measures of complexity obtained from the tibia bone biopsies (0.64 – 0.797), whereas the correlation with 2D histomorphometric measures is considerably lower (-0.649 – 0.663).

Again, this is an indication that the strength of the bone is related to the holistic composition of the bone rather than to single linear measures of the structure. Fig. 19 shows the exponential increasing strength measured by BSI when the 3D complexity of the architectural composition increases linearly.

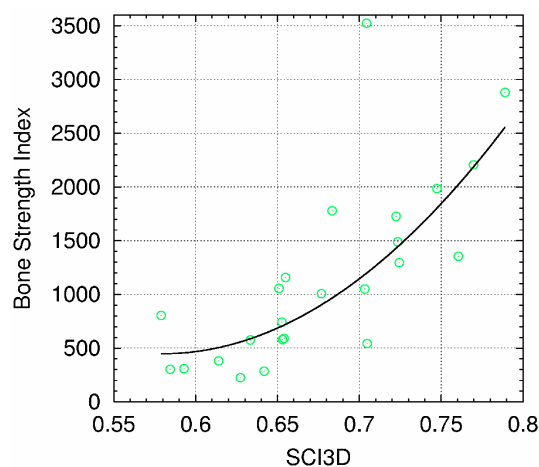


Fig. 19: Relationship between Surface Complexity Index in 3D (SCI3D) and Bone Strength Index (BSI). The BSI increases rapidly with increasing complexity of the architectural composition in 3D. Bones with a high bone strength index are also characterized by an increased value of the complexity of their tissue architecture.

Further statistical work, for instance multi-regression analysis, will be performed and evaluated in the second phase of the project. However, the achievements in regards to the developments of the 3D measures of complexity are promising and provide already new insights to the structural composition of human bones.

## Views and Recommendations from the Industrial Partners

### Siemens AG

Siemens Medical Solutions has been participating in the project over the last two years and supported the research by a donation of about 100 k Euro as well as by participation in regular meetings. The scientific interest by the Computed Tomography Division of Siemens is the characterization of bone structures which goes beyond the traditional Bone Mineral Density parameter used to quantify the extend of osteoporotic disease.

The research work of the project on measures of complexity has led to the development of such parameters in two and three dimensional space. The application to various bone specimens has shown a definite relation between the measures of complexity and the anatomy of bones and thus is the basis of diagnostic interpretation for in vivo applications.

Most modern imaging technologies, like micro-CT, have been used to experimentally check underlying theoretical assumptions and algorithms.

We perceived the cooperation between the partners of the project as very productive and efficient. The individual tasks have been well defined and distributed among the partners. Corresponding results have been exchanged regularly and have been combined to form a complete picture. The regular team meetings between all partners have been an important element to achieve the present level of success.

The application of high resolution multislice CT to volunteers and patients is an interesting continuation of the previous research work to relate the measures of complexity to corresponding stages of disease in vivo.

Signed by Klaus Klingenberg-Regn, PhD; Siemens AG

### Scanco Medical AG

I hereby want to express my thanks for working together in the MAP project AO-99-030 very successfully. The work done so far was very helpful for us in different aspects:

- Access to a larger number of human biopsies/autopsies
- Comparison of our systems to others (image quality)
- Comparison of our software methods to others
- Comparison of our morphometry-results with standard histology
- Fruitful discussions regarding CT-technology.

We therefore think that our work and manpower for this project was paid off by the above facts and we will definitely continue the project if possible.

Signed by Bruno Koller, PhD; SCANCO Medical AG

## Publications

### Scientific Publications

#### 1. Comparison of Bone Loss with Changes of Bone Architecture at Six Different Skeletal Sites Using Measures of Complexity

P. Saporin, W. Gowin, D. Felsenberg  
J. Grav. Physiol. 9, 2002; P177-178

We explore the structural deterioration of human bone tissue in osteoporosis as a model for bone loss in microgravity conditions. Measures of complexity are applied to quantify the structural composition of bone tissue at six different skeletal locations. The complexity of the bone architecture and the rate of its decay during the bone loss are analyzed and compared with each other at the different locations.

#### 2. Visual Analysis of Trabecular Bone Structure

S. Prohaska, H.-C. Hege, M. Giehl, W. Gowin  
J. Grav. Physiol. 9, 2002; P171-172

Acquiring image data of bone biopsies by a micro-CT scanner is today a common technique. The amount of data to be assessed is huge. The task to assess quantitative measures requires a concise visualization. We present visualization techniques that can be used interactively on state-of-the-art PCs and demonstrate how the frontier can be pushed further. A skeletonization process is applied to the image of the bone to create the central surface. After triangulation this surface can be rendered at interactive frame rates. When the surface is additionally colored by local measures (mean grey value of image data, local thickness) the overall structure and details can be recognized at the same time. This can facilitate the exploration of the biopsy and can help finding special features.

#### 3. Bone Modeling and Structural Measures of Complexity

A. Zaikin, J. Kurths, P. Saporin, W. Gowin  
J. Grav. Physiol. 9, 2002; P175-176

We test sensitivity and powerfulness of recently suggested Structure Measures of Complexity (SMC) with simulated test objects, represented by simple structures or modelled on the basis of a real bone image. We check how these SMC react the local and global disordering processes, as well as a deterioration of the bone structure. We show that applications of SMC provide additional information about any changes of the bone structure in comparison to bone mineral density (BMD), and that they can be potentially helpful in the diagnosis of osteoporosis.

#### 4. Fast Visualization of Plane-Like Structures in Voxel Data

S. Prohaska, H.-C. Hege  
IEEE Visualization 2002 (VIS 2002); 29-36

We present a robust, noise-resistant criterion characterizing plane-like skeletons in binary voxel objects. It is based on a distance map and the geodesic distance along the object's boundary. A parameter allows to control the noise sensitivity.

If needed, homotopy with the original object might be reconstructed in a second step, using an improved distance ordered thinning algorithm.

The skeleton is analyzed to create a geometric representation for rendering. Plane-like parts are transformed into a triangulated surface not enclosing a volume by a suitable triangulation scheme.

The resulting surfaces have lower triangle count than those created with standard methods and tend to maintain the original geometry, even after simplification with a high decimation rate. Our algorithm allows to interactively render expressive images of complex 3D structures, emphasizing independently plane-like and rod-like structures.

The methods are applied for visualization of the microstructure of bone biopsies.

### Oral Presentations at Conferences

1. 8<sup>th</sup> European Symposium on Life Sciences Research in Space and the 23<sup>rd</sup> Annual International Gravitational Physiology Meeting, Stockholm, Sweden, June 2002:
  - a. **“Visual Analysis of Trabecular Bone Structure”**  
S. Prohaska, H.-C. Hege, M. Giehl, W. Gowin  
Proceedings of “Life in Space for Life on Earth”, ESA SP-501, pp 75-76
  - b. **“Bone Modeling and Structural Measures of Complexity”**  
A. Zaikin, J. Kurths, P. Saporin, W. Gowin  
Proceedings of “Life in Space for Life on Earth”, ESA SP-501, pp 79-80
  - c. **“Comparison of Bone Loss with Changes of Bone Architecture at Six Different Skeletal Sites Using Measures of Complexity”**  
P. Saporin, W. Gowin, D. Felsenberg  
Proceedings of “Life in Space for Life on Earth”, ESA SP-501, pp 81-82
2. IV. Baltic Bone and Cartilage Conference, Binz, Germany, September 2002:
  - a. **“Femoral Neck Fractures: Reasons for the Most Common Location of the Fractures”**  
W. Gowin, P. Saporin, S. Prohaska, H.-C. Hege, D. Felsenberg  
Acta Orthop Scand (Suppl 304), 73, 2002; 26
3. IEEE Visualization 2002, Boston, USA, October 2002:
  - a. **“Fast Visualization of Plane-Like Structures in Voxel Data”**  
S. Prohaska, H.-C. Hege)  
IEEE Visualization 2002 (VIS 2002); 29-36

### Poster Presentations at Conferences

1. World Congress on Osteoporosis, Lisbon, May 2002:  
**“Regional Structural Skeletal Discordance Assessed by Measures of Complexity”**  
W. Gowin, P. Saporin, D. Felsenberg, J. Kurths, A. Zaikin, S. Prohaska, H.-C. Hege  
Osteoporosis Int 13, 2002; S123
2. IV. Baltic Bone and Cartilage Conference, Binz, Germany, September 2002:  
**“Comparison of bone composition at six different skeletal locations by measures of complexity and bone mineral density”**  
P. Saporin, W. Gowin, D. Felsenberg  
Acta Orthop Scand (Suppl 304), 73, 2002; 48
3. Dynamics Days Europe, Heidelberg, Germany, July 2002:  
**“Bone Modeling and Structural Measures of Complexity”**  
A. Zaikin, P. Saporin, S. Prohaska, J. Kurths, W. Gowin

### Other Scientific Work

A PhD-Thesis based on the work within this project has been issued in 2002 to Stefan Beller, MD, at FUB with the title: **“Comparison and Evaluation of Parameters for the Quantification of Bone Structures in Different Skeletal Regions”** (Promotor: W. Gowin, MD, PhD)

Financial support was received from



and the academic institutions: Free University Berlin (Germany), University of Potsdam (Germany), Konrad-Zuse Institute Berlin (Germany), University of Aarhus (Denmark).